

# Particle freeze-out and discontinuities in relativistic hydrodynamics

K A Bugaev<sup>†‡</sup>, M I Gorenstein<sup>†‡</sup> and W Greiner<sup>†</sup>

<sup>†</sup> Institute for Theoretical Physics, Goethe University, Frankfurt, Germany

<sup>‡</sup> Bogolyubov Institute for Theoretical Physics, Kiev, Ukraine

**Abstract.** Freeze-out of particles in relativistic hydrodynamics is considered across a 3-dimensional space-time hypersurface. The conservation laws for time-like parts of the freeze-out hypersurface require different values of temperature, baryonic chemical potential and flow velocity in the fluid and in the final particle spectra. We analyze this freeze-out discontinuity and its connection to the shock-wave phenomena in relativistic hydrodynamics.

## 1. Introduction

Relativistic hydrodynamical model [1] has been widely discussed in recent years within their connection to high energy nucleus-nucleus (A+A) collisions (see, for example, [2]). This approach is the most straight and unique way to investigate the hadron-matter equation of state (EoS) and possible phase transition into a deconfined state called the quark-gluon plasma. The aim of the relativistic hydrodynamical model of A+A collisions is to elucidate the properties of the highly excited matter comparing the model results with experimental observables. The system evolution in relativistic hydrodynamics is governed by the energy-momentum tensor

$$T^{\mu\nu} = (\varepsilon + p)u^\mu u^\nu - pg^{\mu\nu} \quad (1)$$

and conserved charge currents. The baryonic current,

$$j^\mu = n u^\mu , \quad (2)$$

plays the main role in the applications to A+A collisions. The hydrodynamical description includes the local thermodynamical variables (energy density  $\varepsilon$ , pressure  $p$ , baryonic density  $n$ ) and the collective four-velocity  $u^\mu = (1 - \mathbf{v}^2)^{-1/2}(1, \mathbf{v})$ . The continuous flows are the solutions of the hydrodynamical equations

$$\partial_\mu T^{\mu\nu} = 0 , \quad \partial_\mu j^\mu = 0 , \quad (3)$$

with specified initial conditions. To complete the system of hydrodynamical equations (3) the fluid EoS has to be added as an input  $p = p(\varepsilon, n)$ . It is usually used in a more convenient form of  $p = p(T, \mu_B)$  with temperature  $T$  and baryonic chemical potential  $\mu_B$  as independent variables. Other thermodynamical functions can be found from the following thermodynamical identities ( $s$  is the entropy density):

$$s = \left( \frac{\partial p}{\partial T} \right)_{\mu_B} , \quad n = \left( \frac{\partial p}{\partial \mu_B} \right)_T , \quad \varepsilon = Ts + \mu_B n - p . \quad (4)$$

Besides the fluid EoS and the initial conditions for the fluid evolution the third crucial ingredient of the hydrodynamical model of A+A collisions is the so-called freeze-out (FO) procedure, i.e. the prescription for the calculations of the final hadron observables. Particles which leave the system and reach the detectors are considered via FO scheme, where the frozen-out particles are formed on a 3-dimensional hypersurface in space-time. The FO description has a straight influence on particle momentum spectra and therefore on all hadron observables. During last three years an essential progress has been achieved in the formulation of the FO procedure in relativistic hydrodynamics. A generalization of the well known Cooper-Frye (CF) formula [3] to the case of time-like FO hypersurface was suggested in Ref. [4]. The new formula does not contain negative particle number contributions on time-like FO hypersurface appeared in the CF procedure from those particles which cannot leave the fluid during its hydrodynamical expansion. The FO procedure of Ref. [4] has been further developed in a series of publications [5-10]. Ref. [8] presents also the kinetic approach to the FO problem.

There is a new distinct and unusual feature of the proposed FO procedure. The parameters of the distribution function for the final particles should be different from those in the

fluid to satisfy the conservation laws. The particle emission from the time-like parts of the FO hypersurface looks as a ‘discontinuity’ in the hydrodynamic motion. We call it the FO shock. In the present paper we analyze a connection of this new type of discontinuities to a general problem of shock waves in relativistic hydrodynamics.

## 2. Freeze-out procedure

In the hydrodynamical model of A+A collisions the fluid expansion has to be ended by the correct transformation of the fluid into free streaming hadrons. The most important requirement for this FO procedure is to satisfy energy-momentum and charge conservations during the fluid transition into free final particles. It is assumed that there is a narrow space-time region where the mean free path of the fluid constituents increases rapidly and becomes comparable with the characteristic size of the system. The local thermal equilibrium is supposedly maintained in this intermediate region. In practice, one considers a “zero width” approximation and introduces a FO surface, so that particle distributions remain frozen-out from there on.

In his original paper Landau [1] defined the FO hypersurface by the condition  $T(t, x) = T^*$ , where  $t$  and  $x$  are the time and the space coordinate respectively, and  $T^*$  is the fluid FO temperature chosen to be approximately equal to the pion mass. The FO procedure, first introduced by Milekhin [11], was based on the intuitive physical assumption of isotropic thermal particle spectra in the rest frames of each fluid element. The final hadron observables was then obtained by the Lorentz transformations of these spectra with known hydrodynamical velocities and integration over all fluid elements. The FO procedure was improved further by Cooper and Frye [3] and this method has been used ever since. Final spectrum for  $i$ -th type hadron is expressed by formula [3]:

$$k^\circ \frac{d^3 N_i}{dk^3} = \frac{d_i}{(2\pi)^3} \int_{\Sigma_f} d\sigma_\mu k^\mu \phi_i \left( \frac{k^\nu u_\nu - \mu_i}{T^*} \right), \quad (5)$$

where  $d\sigma_\mu$  is the external normal 4-vector to the FO hypersurface  $\Sigma_f$ ,  $\phi_i$  denotes the local thermal Bose or Fermi distributions,  $d_i$  is the degeneracy factor for particle  $i$  with the chemical potential  $\mu_i$ . The particle spectrum (5) is known as the Cooper-Frye (CF) distribution function. The chemical potential  $\mu_i$  is equal to

$$\mu_i = b_i \mu_B + s_i \mu_S + q_i \mu_Q, \quad (6)$$

where  $b_i, s_i, q_i$  are the baryonic number, strangeness and electric charge of  $i$ -th particle. The strange chemical potential  $\mu_S$  and electric chemical potential  $\mu_Q$  are always chosen to make the total strangeness to be equal to zero and the ratio of electric charge to the baryonic number to be fixed at their initial value given by A+A collision. Therefore, only the baryonic chemical potential  $\mu_B$  is considered as independent thermodynamical variable.

The CF formula (5) corrected the Milekhin’s approach. The matter is that the external normal vector  $d\sigma_\mu$  equal to  $(-dx, dt)$  in 1+1 dimensions does not in general become equal to  $d\sigma_\mu^* = (-dx^*, 0)$  after the Lorentz transformation into the fluid element rest frame. The non-simultaneous particle FO in the rest frame of the fluid element modifies the thermal distribution function and causes a nonzero momentum of the fluid element in its rest frame (“local anisotropy”, see Ref. [12] for details).

The initial conditions of the hydrodynamical motion are given on the initial hypersurface  $\Sigma_{in}$ . The final hypersurface  $\Sigma_f$  should be closed to  $\Sigma_{in}$  and in general  $\Sigma_f$  consists of both space-like (s.l.) and time-like (t.l.) parts. Using the Gauss theorem and Eq. (3) one can easily prove the energy-momentum and charge number conservations with CF FO formula:

$$\int_{\Sigma_{in}} d\sigma_\mu T^{\mu\nu} = \int_{\Sigma_f} d\sigma_\mu T^{\mu\nu} \equiv \sum_i \frac{d_i}{(2\pi)^3} \int_{\Sigma_f} d\sigma_\mu \int \frac{d^3k}{k^0} k^\mu k^\nu \phi_i \left( \frac{k_\lambda u^\lambda - \mu_i}{T^*} \right), \quad (7)$$

$$\int_{\Sigma_{in}} d\sigma_\mu j^\mu = \int_{\Sigma_f} d\sigma_\mu j^\mu \equiv \sum_i \frac{d_i b_i}{(2\pi)^3} \int_{\Sigma_f} d\sigma_\mu \int d^3k k^\mu \phi_i \left( \frac{k_\lambda u^\lambda - \mu_i}{T^*} \right), \quad (8)$$

where  $b_i$  is the baryonic number of  $i$ -th particle and the summation over all particles and the corresponding antiparticles is assumed in the right hand side of Eqs. (7,8). Note that fluid EoS at the FO is assumed to be an ideal gas EoS for a mixture of different particle species. The hydrodynamical quantities  $T^{\mu\nu}$  (1) and  $j^\mu$  (2) are identically presented on the FO surface  $\Sigma_f$  in terms of final particle distributions  $\phi_i$  according to Eqs. (7,8).

The CF formula (5) still does not provide a complete solution of the FO problem. The FO surface consists of t.l. parts too. Eq. (5) can not however be used for a t.l. FO surface (i.e., s.l. normal vector  $d\sigma_\mu$ ): free final particles “return” to the fluid if  $d\sigma_\mu k^\mu < 0$ , and this causes unphysical *negative* contributions to the *number* of final particles. A first attempt to improve the CF formula for t.l. FO hypersurface was done by Sinyukov in Ref. [13]. The modified FO procedure and new formula for the final particle spectra emitted from the t.l. FO hypersurface was proposed in Ref. [4]:

$$k^0 \frac{d^3 N_i}{dk^3} = \frac{d_i}{(2\pi)^3} \int_{\Sigma_f} d\sigma_\mu k^\mu \phi_i \left( \frac{k_\lambda u_g^\lambda - \mu_i^g}{T_g} \right) \theta(d\sigma_\nu k^\nu). \quad (9)$$

Eq. (9) looks like CF formula (5), but without negative particle numbers that appear in (5) for t.l. FO surfaces. These negative contributions are cut-off by the  $\theta$ -function in Eq. (9). We’ll call Eq. (9) the cut-off (CO) distribution in what follows. An inclusion of the CO FO into the self-consistent hydrodynamical scheme is considered in Ref. [10]. The distribution function for the free particles in Eq. (9) contains the new parameters  $T_g, \mu_i^g, u_g^\nu$ . We’ll briefly call the free particle state as the ‘gas’ in order to distinguish it from the ordinary fluid. Note, however, that final particle system differs from the normal fluid and gas. It has the non-thermal CO distribution function which is frozen-out as all further particle rescatterings are ‘forbidden’ in the post-FO gas state.

The conservation laws across FO hypersurface  $\Sigma_f$  can be written now in their local form as

$$\begin{aligned} & \sum_i \frac{d_i}{(2\pi)^3} d\sigma_\mu \int \frac{d^3k}{k^0} k^\mu k^\nu \phi_i \left( \frac{k_\lambda u_f^\lambda - \mu_i^f}{T_f} \right) \\ = & \sum_i \frac{d_i}{(2\pi)^3} d\sigma_\mu \int \frac{d^3k}{k^0} k^\mu k^\nu \phi_i \left( \frac{k_\lambda u_g^\lambda - \mu_i^g}{T_g} \right) \theta(d\sigma_\nu k^\nu), \end{aligned} \quad (10)$$

$$\sum_i \frac{d_i b_i}{(2\pi)^3} d\sigma_\mu \int d^3k k^\mu \phi_i \left( \frac{k_\lambda u_f^\lambda - \mu_i^f}{T_f} \right) \quad (11)$$

$$= \sum_i \frac{d_i b_i}{(2\pi)^3} d\sigma_\mu \int d^3k k^\mu \phi_i \left( \frac{k_\lambda u_g^\lambda - \mu_i^g}{T_g} \right) \theta(d\sigma_\nu k^\nu) .$$

These conservation laws were derived together with the equation of motion of the fluid in Ref. [10] and should be solved simultaneously with the latter ones in order to find the FO hypersurface in the practical hydrodynamical calculations.

The presence of the  $\theta$ -function in the right hand side of Eqs. (10,11) leads to the discontinuity between the fluid  $T_f, \mu_i^f, u_f^\nu$  and the gas  $T_g, \mu_i^g, u_g^\nu$  variables to satisfy the energy-momentum and baryonic number conservation. We call this discontinuity the FO shock. Note that the strangeness flow across the FO surface is equal to zero and electric charge flow is proportional to the baryonic number flow. Therefore, the conservation of strangeness and electric charge is also fulfilled.

Another FO discontinuity problem occurs in the hydrodynamical model calculations when the EoS is different on the two sides of the FO front (for the final gas of free particles one must use the ideal gas distributions). The conservation laws on the FO surface in this case should lead to the discontinuities between fluid and gas of final particles across both t.l. and s.l. parts of  $\Sigma_f$  [14]. The discontinuity across the s.l. part of  $\Sigma_f$  corresponds to the so-called time-like shocks [15] (i.e.,  $d\sigma_\mu$  is t.l. vector) and will be also discussed in the next Sections.

### 3. Relativistic shock waves

Equations (3) are the differential form of the energy-momentum and baryonic number conservation laws. Along with these continuous flows, the conservation laws can also be realized in the form of discontinuous hydrodynamical flows which are called shock waves and satisfy the following equations:

$$T_o^{\mu\nu} \Lambda_\nu = T^{\mu\nu} \Lambda_\nu \quad , \quad n_o u_o^\mu \Lambda_\mu = n u^\mu \Lambda_\mu \quad , \quad (12)$$

where  $\Lambda_\mu$  is the unit 4-vector normal to the discontinuity hypersurface. In Eq. (12) the zero subscript corresponds to the initial state ahead of the shock front and the quantities without an index are the final state values behind it.

The important constraint on the transitions (12) is the requirement of non-decreasing entropy (thermodynamical stability condition):

$$s u^\mu \Lambda_\mu \geq s_o u_o^\mu \Lambda_\mu \quad . \quad (13)$$

We consider one-dimensional hydrodynamical motion in what follows. In its usual sense the theory of the shock waves corresponds to the discontinuities on the surface with space-like  $\Lambda_\mu$ , i.e., the shock-front velocity is smaller than 1. In this case one can always choose the Lorentz frame where the shock front is at rest. Then the hypersurface of shock discontinuity is  $x_{sh} = const$  and  $\Lambda_\mu = (0, 1)$ . The shock equations (12) become

$$T_o^{01} = T^{01}, \quad T_o^{11} = T^{11} \quad , \quad n_o u_o^1 = n u^1 \quad . \quad (14)$$

From Eq. (14) one obtains

$$v_o^2 = \frac{(p - p_o)(\varepsilon + p_o)}{(\varepsilon - \varepsilon_o)(\varepsilon_o + p)} \quad , \quad v^2 = \frac{(p - p_o)(\varepsilon_o + p)}{(\varepsilon - \varepsilon_o)(\varepsilon + p_o)} \quad . \quad (15)$$

Substituting (15) into the last equation in (14) we obtain the well known Taub adiabat (TA) equation [16]

$$n^2 X^2 - n_o^2 X_o^2 - (p - p_o)(X + X_o) = 0 , \quad (16)$$

in which  $X \equiv (\varepsilon + p)/n^2$ , and TA therefore contains only the thermodynamical variables.

Eq. (16) can be written also in the form

$$n^2 = n_o^2 \frac{(\varepsilon + p_o)(\varepsilon + p)}{(\varepsilon_o + p_o)(\varepsilon_o + p)} . \quad (17)$$

If the equation of state  $p = p(\varepsilon, n)$  is given, then Eq. (17) defines the function  $n = n_T(\varepsilon)$  which is the TA (16) in the  $(\varepsilon, n)$  plane. The TA in the  $(\varepsilon, p)$  plane is defined by the function  $p_T(\varepsilon) = p(\varepsilon, n_T(\varepsilon))$ . In the case of zero baryonic number it is just reduced to the EoS  $p_T(\varepsilon) = p(\varepsilon)$ . The point  $(\varepsilon_o, p_o, n_o)$  is called the center of the TA. The shock transition from the state  $(\varepsilon_o, p_o, n_o)$  to  $(\varepsilon_1, p_1, n_1)$  is mechanically stable if for all  $\varepsilon$  between  $\varepsilon_o$  and  $\varepsilon_1$  the following inequality is valid [17]:

$$(\varepsilon_1 - \varepsilon_o) [p_{cr}(\varepsilon) - p_T(\varepsilon)] \geq 0 , \quad (18)$$

where

$$p_{cr}(\varepsilon) = A - \frac{C}{A + \varepsilon} \quad (19)$$

with

$$A = \frac{\varepsilon_1 p_1 - \varepsilon_o p_o}{\varepsilon_1 - \varepsilon_o + p_o - p_1} , \quad C = (A + \varepsilon_o)(A - p_o) = (A + \varepsilon_1)(A - p_1) . \quad (20)$$

Thermodynamical stability (13) follows from the mechanical stability (18), and the inverse statement is not in general true [17]. It follows from (18) that the necessary and sufficient condition for the mechanical stability of shocks is that the compression ( $\varepsilon_1 > \varepsilon_o$ ) TA  $p_T(\varepsilon)$  goes under the critical curve  $p_{cr}(\varepsilon)$  (19) and the rarefaction ( $\varepsilon_1 < \varepsilon_o$ ) TA goes above  $p_{cr}(\varepsilon)$  for all  $\varepsilon$  between the initial  $\varepsilon_o$  and final  $\varepsilon_1$  points. The consequences of these relations are the well-known inequalities for the speed of sound,  $c_s = [(\partial p / \partial \varepsilon)_{s/n}]^{1/2}$ , and the flow velocities at both sides of the shock front in its rest frame

$$c_{s0} \leq v_0 , \quad c_{s1} \geq v_1 , \quad (21)$$

which are the necessary conditions of the general mechanical stability criterion (18).

The function

$$z_T(\varepsilon) = \frac{d^2 p_T}{d\varepsilon^2} + \frac{2}{\varepsilon + p_T} \frac{dp_T}{d\varepsilon} \left( 1 - \frac{dp_T}{d\varepsilon} \right) . \quad (22)$$

defines the thermodynamic properties, i.e., the medium is said to be thermodynamically normal if the quantity  $z_T$  is positive, and thermodynamically anomalous when  $z_T < 0$ . In the normal case  $z_T > 0$  the compression shocks are stable whereas the rarefaction shocks become stable in the thermodynamically anomalous media with  $z_T < 0$ . Note that the function  $p_{cr}(\varepsilon)$  (19) is the solution of the equation  $z_T(\varepsilon) = 0$ . The case of varying sign of  $z_T(\varepsilon)$  which is typical for the phase transitions are discussed in Refs. [19, 20].

Let us consider now the discontinuities on a hypersurface with a t.l. normal vector  $\Lambda_\mu$ . This possibility was suggested by Csernai in Ref. [15]. We call them t.l. shocks. In this case

one can always choose another convenient Lorentz frame ('simultaneous system') where the hypersurface of the discontinuity is  $t_{sh} = const$  and  $\Lambda_\nu = (1, 0)$ . Equations (12) become then

$$T_o^{00} = T^{00}, \quad T_o^{10} = T^{10}, \quad n_o u_o^0 = n u^0. \quad (23)$$

From Eq. (23) we find

$$\tilde{v}_o^2 = \frac{(\varepsilon - \varepsilon_o)(\varepsilon_o + p)}{(p - p_o)(\varepsilon + p_o)}, \quad \tilde{v}^2 = \frac{(\varepsilon - \varepsilon_o)(\varepsilon + p_o)}{(p - p_o)(\varepsilon_o + p)}, \quad (24)$$

where we use “ $\sim$ ” sign to distinguish the t.l. shock case (24) from the standard s.l. shocks (15). Substituting (24) into the last equation in (23) one finds the equation for t.l. shocks which is identical to the TA of Eq. (16). We stress, however, that the intermediate steps are quite different. The two solutions, Eqs. (24) and (15), are connected to each other by simple relations,

$$\tilde{v}_o^2 = \frac{1}{v_o^2}, \quad \tilde{v}^2 = \frac{1}{v^2}, \quad (25)$$

between the velocities of s.l. and t.l. shocks. These relations show that only one type of transitions can be realized for the given initial and final states. Physical regions  $[0, 1)$  for  $v_o^2, v^2$  (15) and for  $\tilde{v}_o^2, \tilde{v}^2$  (24) can be easily found in the  $(\varepsilon-p)$ -plane shown in Fig. 1.

If one takes as the initial and final states only states which are thermodynamically equilibrated, the TA passes then through the center of TA  $(\varepsilon_o, p_o)$ . For any physical EoS with  $0 \leq c_s \leq 1$  TA lies as a whole in the regions I and IV in Fig. 1 [18], i.e. only compression and/or rarefaction s.l. shocks (with s.l. normal vector  $\Lambda_\mu$ ) are permissible.

The only way to make the t.l. shocks to be possible is to allow the metastable initial and/or final states. The TA then no longer passes through the initial point  $(\varepsilon_o, p_o)$  and new possibilities of t.l. shock transitions (23,24) to regions III and VI in Fig. 1 would be realized (see, e.g., the t.l. shock hadronization of supercooled quark-gluon plasma in Ref. [21]).

#### 4. Freeze out shocks

The conservation laws (10,11) between the fluid and the free streaming particles are simplified across the s.l. FO hypersurface. In this case the  $\theta$ -function in the right hand side of Eqs. (10,11) is equal to unity for all momenta of final particles. The CO formula (9) is reduced to the CF distribution (5) at s.l. parts of the FO hypersurface. It was shown in the previous Section that t.l. shocks (shocks across s.l. hypersurface) are not permissible for any physical EoS, in particular for the ideal gas EoS for the fluid and the gas of free particles. It means that the only solution of Eqs. (10,11) is

$$T_f = T_g, \quad \mu_i^f = \mu_i^g, \quad u_f^\mu = u_g^\mu. \quad (26)$$

No discontinuities between the fluid and the gas parameters can exist, and the particle emission from s.l. hypersurface is a smooth FO according to the CF formula (5). We do not discuss here the possibilities when the fluid FO takes place from the state which is out of local thermodynamical equilibrium.

For the t.l. parts of the FO hypersurface  $\Sigma_f$  a rather different solution should be realized. The  $\theta$ -function in Eqs. (10,11) equals to zero when  $d\sigma_\nu k^\nu$  is negative. Therefore the smooth

solution (26) for Eqs. (10,11) does not exist. In this case the only possibility to satisfy the conservation laws (10,11) is to introduce a discontinuity between the fluid  $T_f, \mu_i^f, u_f^\mu$  and gas  $T_g, \mu_i^g, u_g^\mu$  parameters. Let us consider this FO shock on t.l. hypersurface in more detail. To obtain the analytical solution of the problem we restrict ourself to the case of zero baryonic number  $n = 0$  and consider massless particles with the Jütner distribution function

$$\phi\left(\frac{k_\mu u^\mu}{T}\right) = \exp\left(-\frac{k_\mu u^\mu}{T}\right). \quad (27)$$

Similar problem, but for the conserved particle number (not the charge!), was considered in Ref. [7].

Substituting it into both sides of the Eq. (10), one finds that the energy-momentum conservation between the fluid and free particles along the t.l. hypersurface acquires the form:

$$\begin{aligned} d\sigma_\mu T_f^{\mu\nu} &\equiv d\sigma_\mu \int \frac{d^3k}{k^0} k^\mu k^\nu \phi\left(\frac{k_\nu u_f^\nu}{T_f}\right) = \\ &= d\sigma_\mu T_g^{\mu\nu} \equiv d\sigma_\mu \int \frac{d^3k}{k^0} k^\mu k^\nu \phi\left(\frac{k_\nu u_g^\nu}{T_g}\right) \theta(d\sigma_\lambda k^\lambda). \end{aligned} \quad (28)$$

The energy-momentum tensor  $T_f^{\mu\nu}$  in Eq. (28) has the form of Eq. (1) with the functions  $\varepsilon(T_f) = \varepsilon_f$  and  $p(T_f) = p_f$  given by

$$\varepsilon(T) = 3p(T) = \frac{1}{2\pi^2} \int_0^\infty k^2 dk k \exp\left(-\frac{k}{T}\right) = \frac{3}{\pi^2} T^4. \quad (29)$$

In the rest frame of the FO front, i.e. in the Lorentz frame where  $d\sigma_\mu$  becomes equal to  $(0, dt)$ , the  $T_g^{01}$  and  $T_g^{11}$  components of the gas energy-momentum tensor in Eq. (28) can be rewritten then in the form

$$T_g^{01} = (\varepsilon_g^* + p_g^*) u_g^0 u_g^1, \quad T_g^{11} = (\varepsilon_g^* + p_g^*) u_g^1 u_g^1 + p_g^*. \quad (30)$$

Note that such a representation can be given only for the  $T_g^{\mu\nu}$  components which enter the energy-momentum conservation (28). This form coincides with that of Eq. (1), but with effective values of  $\varepsilon_g^*$  and  $p_g^*$  which are found to be equal to

$$\varepsilon_g^* = \varepsilon(T_g) \frac{(1 + v_g)^2}{4v_g}, \quad p_g^* = p(T_g) \frac{(1 + v_g)^2(2 - v_g)}{4}, \quad (31)$$

where  $v_g$  is the velocity parameter of the gas in the FO shock rest frame. The functions  $\varepsilon$  and  $p$  in the right hand side of Eqs. (31) are given by Eq. (29).

Due to the same formal structure of  $T_g^{01}, T_g^{11}$  (30) and  $T_f^{01}, T_f^{11}$  (1) one obtains the solution of Eq. (28)

$$v_f^2 = \frac{(p_f - p_g^*)(\varepsilon_g^* + p_f)}{(\varepsilon_f - \varepsilon_g^*)(\varepsilon_f + p_g^*)}, \quad v_g^2 = \frac{(p_f - p_g^*)(\varepsilon_f + p_g^*)}{(\varepsilon_f - \varepsilon_g^*)(\varepsilon_g^* + p_f)}, \quad (32)$$

which is similar to Eq. (15). Note, however, that in contrast to Eq. (15) the values of  $\varepsilon_g^*$  and  $p_g^*$  in Eq. (32) are not just the thermodynamical quantities, but depend also on  $v_g$ .



It should be emphasized that Eq. (30) can also be introduced for the distribution functions of massive and charged particles [10]. In the latter case the energy-momentum conservation leads to the familiar expressions (32) for the effective energy density and pressure, and the charge conservation leads to the TA equation (16) or (17) for the effective charge density.

We fix the FO hypersurface  $\Sigma_f$  by the condition  $T_g = \text{const.}$  The analytical solution of Eq. (32) can be presented then in the form

$$v_g = \frac{9v_f^2 - 8v_f + 3}{3v_f^2 + 1}, \quad R \equiv \left(\frac{T_f}{T_g}\right)^4 = \frac{4(3v_f^2 - 2v_f + 1)^2(v_f + 1)}{(3v_f - 1)(3v_f^2 + 1)^2}. \quad (33)$$

It is instructive to compare these results with shock-wave solution (15) for the same ideal gas EoS (29). We fix the temperature  $T_g$  of the final state in s.l. shock wave (14) and consider  $v_g$  and  $T_f$  dependence on  $v_f$ :

$$v_g = \frac{1}{3v_f}, \quad R \equiv \left(\frac{T_f}{T_g}\right)^4 = \frac{3(1 - v_f^2)}{9v_f^2 - 1}. \quad (34)$$

Figs. 2 and 3 show the dependences of  $v_g$  and  $T_f$  on  $v_f$  for the fixed value of  $T_g$  in the final state, both for the FO shock (33) and for the normal shock wave (34). The kinematical restrictions on the gas velocity give the same value of the minimal fluid velocity in both shock transitions,  $(v_f)_{\min} = p_f/\varepsilon_f$ . It equals to  $1/3$  for the considered ideal gas EoS (29) for the fluid. Figs. 2 and 3 indicate that at low values of the fluid velocity,  $v_f < 1/\sqrt{3}$ , the behavior of  $v_f$  and  $T_f/T_g$  for the FO shock (33) and for the normal shock wave (34) is quite similar. The value of  $v_f = 1/\sqrt{3}$  corresponds to the speed of sound,  $c_s = 1/\sqrt{3}$ , in the system with ideal gas EoS (29). According to the requirements given by Eq. (21) the shock transitions at  $v_f < c_s$  are mechanically unstable. Mechanically stable solutions at  $v_f > c_s$  for normal shock waves and FO shocks have qualitatively different behavior. For the stable normal shock wave one has  $v_g < v_f$  and  $T_f < T_g$  (see Figs. 2, 3), i.e. only compression normal shock wave transitions ' $f \rightarrow g$ ' would be stable. For the FO shock transitions we find a completely different behavior,  $v_g > v_f$  and  $T_f > T_g$ , illustrated in Figs. 2, 3. In contrast to the normal shock waves, only the rarefaction FO shock transitions ' $f \rightarrow g$ ' are stable. This result is in agreement with an intuitive physical picture of the FO as a rarefaction process.

The decompression degree in the FO shock can be estimated by the energy density ratio on both side of the discontinuity. In Appendix B of Ref. [10] the energy density of the gas was found according to the Landau-Lifshitz definition of the collective velocity [22]. In order to find the desired quantity it is necessary to diagonalize the energy-momentum tensor of the gas by the Lorentz transformation. Zero-zero component of the obtained tensor is the energy density. It is found to be smaller than the effective energy density  $\varepsilon_g^*$  and is given by

$$T_g^{00}(v_g, T_g)\Big|_{L.L.} = \varepsilon(T_g) \left(1 - \frac{\Delta}{2}\right)^2 \frac{\left(\sqrt{4 + 2\Delta + \Delta^2} + 1 + \Delta\right)}{3}, \quad (35)$$

where  $\Delta \equiv 1 - v_g$  and  $v_g$  is defined by Eq. (33). The magnitude of decompression in the FO shock is presented in Fig. 4. It reaches the maximal value of about 2 at the edge of of the stability region,  $v_f = 1/\sqrt{3}$ . Therefore, the quantitative change of the hydrodynamical values in the FO shock is not negligible and it might be manifested in the various applications.

The entropy flux of the fluid is given by

$$s_f^\mu d\sigma_\mu = s_f u_f^\mu d\sigma_\mu, \quad (36)$$

where  $s_f = (\varepsilon_f + p_f)/T_f$  is the fluid entropy density. Similar expression is valid for the final 'gas' state in the case of normal shock waves. The entropy production in the normal shock waves is given by the formula

$$\frac{s_g^\mu d\sigma_\mu}{s_f^\mu d\sigma_\mu} = \frac{1}{3^{3/4} v_f} \left[ \frac{9v_f^2 - 1}{1 - v_f^2} \right]^{1/4}, \quad (37)$$

shown in Fig. 5. The entropy flux of the gas with the cut-off distribution function is given by [10]:

$$s_g^\mu d\sigma_\mu = \int \frac{d^3k}{k^0} k^\mu d\sigma_\mu \phi \left( \frac{k_\nu u_g^\nu}{T_g} \right) \left[ 1 - \ln \phi \left( \frac{k_\nu u_g^\nu}{T_g} \right) \right] \theta(d\sigma_\lambda k^\lambda). \quad (38)$$

The entropy production in the FO shocks is calculated then as

$$\frac{s_g^\mu d\sigma_\mu}{s_f^\mu d\sigma_\mu} = \frac{1}{2v_f} \left[ \frac{(3v_f^2 + 1)^2 (1 - 3v_f)}{(1 + v_f)} \right]^{1/4}. \quad (39)$$

The maximal entropy production in the FO shock (39) corresponds to  $v_f = c_s = 1/\sqrt{3}$  and can be considered as an analog of the Chapman–Jouguet point. One has to note that the Chapman–Jouguet point of the FO shock is also the boundary of the mechanical stability. It is similar to the case of the usual shocks [17, 18, 19, 20, 23].

The initial  $(\varepsilon_f, p_f)$  values in the FO shock belong to the straight line  $p = \varepsilon/3$  in the  $\varepsilon$ – $p$  plane. The respective final effective values  $(\varepsilon_g^*, p_g^*)$  are defined by the energy-momentum conservation (30). For the fixed FO temperature ( $T_g = \text{const}$ ) the possible values of  $(\varepsilon_f, p_f)$  and the corresponding values of  $(\varepsilon_g^*, p_g^*)$  are shown in Fig. 6. The point O in Fig. 6 corresponds to  $v_f \rightarrow 1$ . It follows that  $v_g \rightarrow 1$  as well and the non-cut distribution function of the gas becomes identical to the fluid one. If the fluid velocity decreases, the gas velocity decreases also. The difference between the fluid and the gas becomes then more pronounced. This leads to a small growth of the gas effective energy (on the arc OB) and an essential growth of the fluid energy density (on the interval OA). The point A is the Chapman–Jouguet point, which corresponds to the maximal value of the effective energy density of the gas. The unstable final states also belong to the same arc BO, but they correspond to the opposite direction of changes. The point A is the mechanically stable initial state of the fluid with maximal energy density. The mechanically unstable initial states are located to the right hand side of the point A.

Curve AOB in Fig. 6 is not a usual TA. The principal difference is that the gas temperature is fixed by the FO condition and there are no states with intermediate temperatures between the given initial and final ones. However, the mechanical stability condition (18) corresponds exactly to the case of usual shocks and TA. The critical curve (19) for points A and B in Fig. 6 is a tangent to the line OA at point A. The stable FO shock transitions satisfy the mechanical stability criterion. For the unstable FO shocks the critical curve has

the intersection point with the line  $p = \varepsilon/3$  within the interval OA. Suppose there is such an intersection point D for the FO shock transition from the initial state C to the final state E of the arc BO in Fig. 6. Then Fig. 5 demonstrates that entropy production on the DE interval is smaller than that on the interval AB. Moreover, the rarefaction shock transition C→D is unstable because it connects the two states of the thermodynamically normal matter. Therefore in the C→D transition the entropy decreases. Combining both results together, one finds that the tangent point A of the critical curve corresponds to the maximum of the entropy production, i.e., it is a Chapman-Jouguet point.

## 5. Summary

In the present paper the particle freeze-out in relativistic hydrodynamics was considered. For time-like parts of the FO hypersurface it is described by the cut-off distribution function and particle emission looks as a discontinuity in the hydrodynamical motion (FO shocks). The connection of these FO shocks to the normal shock waves in the relativistic hydrodynamics has been analyzed.

The FO shock transition of the fluid to the gas of free particles with the cut-off distribution function is mechanically stable if the fluid velocity  $v_f$  in the rest frame of the FO shock front is larger than the speed of sound  $c_s$  inside the fluid. This condition coincides with the mechanical stability criteria for the normal shock waves. In this case the particle emission does not influence the fluid evolution and can be selfconsistently included in the relativistic hydrodynamical models. We have used only the consequence (21) of the mechanical stability condition. Its complete formulation for the t.l. F.O. requires further studies.

Analytical solution for the FO shocks are obtained in the case of the ideal gas EoS (29). In contrast to the normal shock waves, FO shocks are found to be the rarefaction shocks:  $T_g < T_f$  and also  $p_g^* < p_f$ ,  $\varepsilon_g^* < \varepsilon_f$ . For the normal shock waves such behavior corresponds to the matter with anomalous thermodynamical properties. The entropy increase (thermodynamical stability) takes place for the rarefaction FO shocks, but the entropy production (39) appears to be quite small.

The FO procedure across a time-like hypersurface considered in this paper could have rather wide field of applications. It is necessary for a correct transformation of hydrodynamical quantities into the spectra of produced particles. One example is the model of A+A collisions which combines hydrodynamics for the early deconfined stage of the reaction with a microscopic non-equilibrium model for the later hadronic stage (see Ref. [24]).

## Acknowledgments

Authors thank D.H. Rischke and Granddon Yen for useful discussions. M.I.G. acknowledges the financial support of DFG, Germany. K.A.B. is grateful to the Alexander von Humboldt Foundation for the financial support.

## References

- [1] Landau L D 1953 *Izv. Akad. Nauk SSSR* **17** 51
- [2] Stöcker H and Greiner W 1986 *Phys. Rep.* **137** 277;  
Clare R B and Strottman D D 1986 *Phys. Rep.* **141** 177;  
Rischke D H 1998 Fluid Dynamics for Relativistic Nuclear Collisions, Proceedings of the Summer School in Theoretical Physics, Cape Town, February 4-13, 1998, p49; Preprint nucl-th/9809044
- [3] Cooper F and Frye G 1974 *Phys. Rev. D* **10** 186
- [4] Bugaev K A 1996 *Nucl. Phys. A* **606** 559
- [5] Neumann J J, Lavrenchuk B and Fai G 1997 *Heavy Ion Physics* **5** 27
- [6] Csernai L P, Lázár Z and Molnár D 1997, *Heavy Ion Physics* **5** 467
- [7] Anderlik Cs, Csernai L P, Grassi F, Hama Y, Kodama T and Lázár Zs 1999 *Phys. Rev. C* **59** 3309
- [8] Anderlik Cs, Lázár Zs, Magas V K, Csernai L P, Stöcker H and Greiner W 1999 *Phys. Rev. C* **59** 1
- [9] Magas V 1999 *Freeze out in hydrodynamical models, Master of Science Thesis, University of Bergen, January 1999*
- [10] Bugaev K A and Gorenstein M I 1999 *Preprint nucl-th/9903072*.
- [11] Milekhin G A 1959 *Zh. Eksp. Teor. Fiz.* **35** 1185; 1959 *Sov. Phys. - JETP* **35** 829; 1961 *Trudy FIAN* **16** 51
- [12] Gorenstein M I and Sinyukov Y M 1984 *Phys. Lett. B* **142** 425
- [13] Sinyukov Y M 1989 *Sov. Nucl. Phys.* **50** 228; 1989 *Z. Phys. C* **43** 401
- [14] Gorenstein M I 1990 *Univ. of Frankfurt preprint, UFTP 251/1990*
- [15] Csernai L 1987 *Zh. Eksp. Teor. Fiz. (Russ.)* **92** 379; 1987 *Sov. Phys. JETP* **65** 216
- [16] Taub A H 1948 *Phys. Rev.* **74** 328
- [17] Gorenstein M I and Zhdanov V I 1987 *Z. Phys. C* **34** 79  
Bugaev K A and Gorenstein M I 1987 *J. Phys. G* **13** 1231  
Bugaev K A and Gorenstein M I 1989 *Z. Phys. C* **43** 261
- [18] Bugaev K A, Gorenstein M I and Zhdanov V I 1988 *Z. Phys. C* **39** 365
- [19] Bugaev K A, Gorenstein M I, Kämpfer B and Zhdanov V I 1989 *Phys. Rev. D* **40** 2983
- [20] Bugaev K A, Gorenstein M I and Rischke D H 1991 *Phys. Lett. B* **255** 18; 1990 *JETP Pis'ma (Russ.)* **52** 1121

- [21] Csörgö T and Csernai L P 1994 *Phys. Lett. B* **333** 494  
Gorenstein M I, Miller H G, Quick R M and Ritchie R A 1994 *Phys. Lett. B* **340** 109
- [22] de Groot S R, van Leeuwen W A and van Weert Ch G 1980 *Relativistic Kinetic Theory*, North-Holland Publishing Company, Amsterdam
- [23] Bugaev K A 1989 *Rarefaction Shocks in Quark Baryonic Matter Hadronization*, Preprint ITP-88-169P, Kiev 11 p
- [24] Bass S A et al. 1999 *Hadronic freeze-out following a first order hadronization in ultra-relativistic heavy-ion collisions*, Preprint nucl-th/9902062

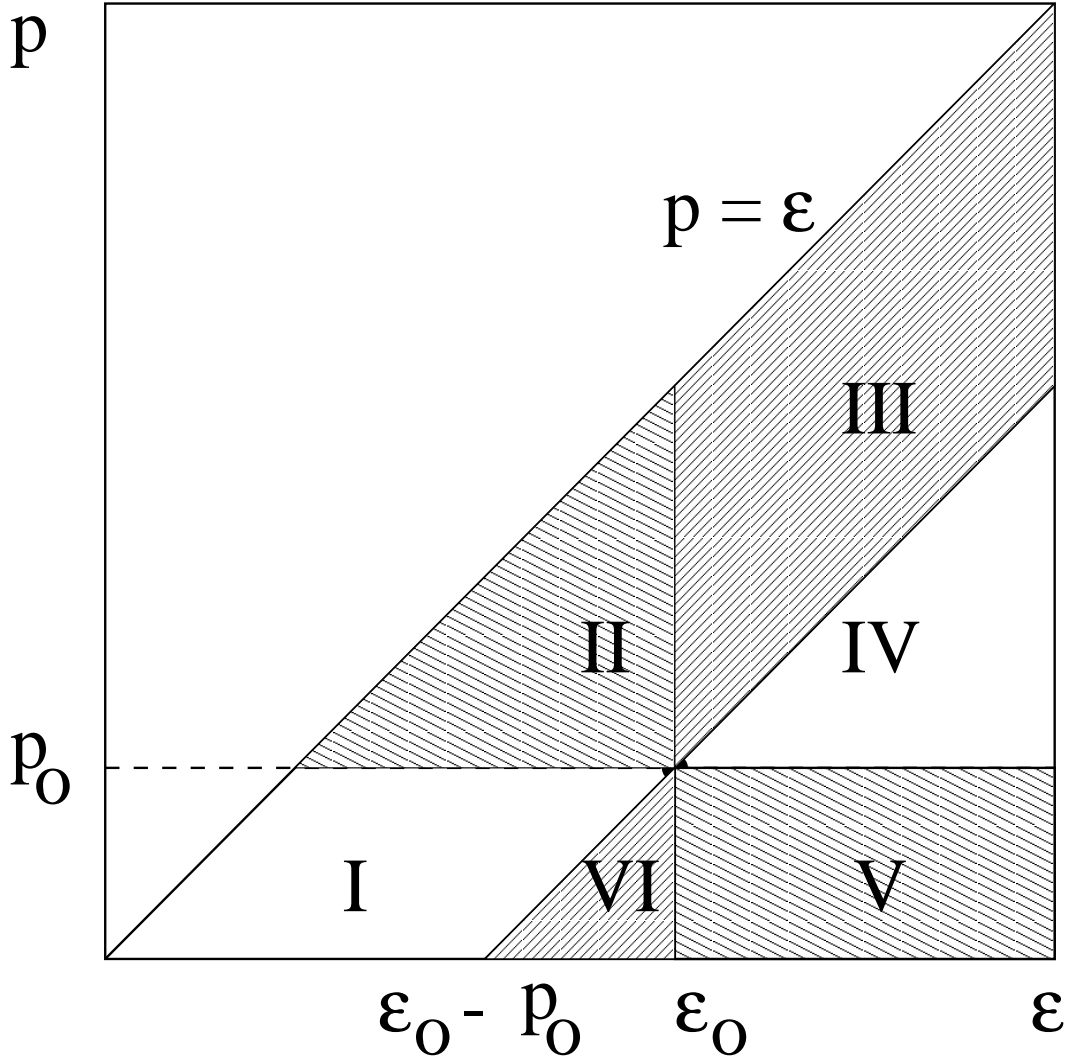


**Fig. 1.** Possible final states in the  $\varepsilon - p$  plane for shock transitions from the initial state  $(\varepsilon_0, p_0)$ . I and IV are the physical regions for s.l. shocks, III and VI for t.l. shocks. II and V are unphysical regions for both types of shocks. Note, that only states with  $p \leq \varepsilon$  are possible for any physical equation of state in relativistic theory.

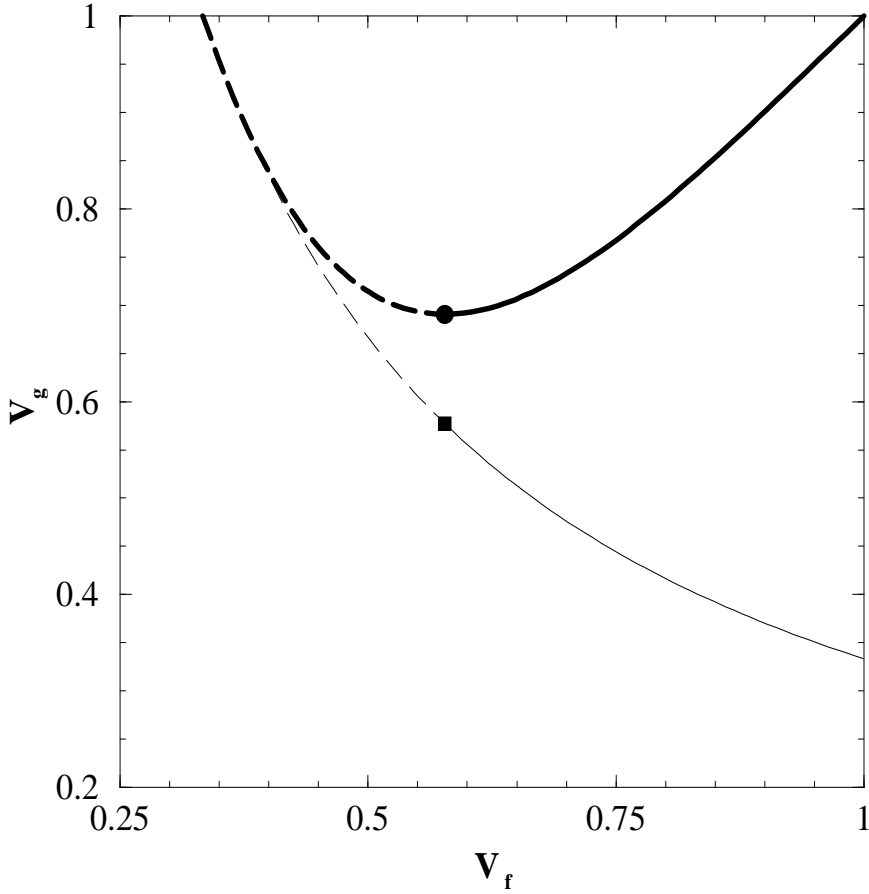


**Fig. 2.** Gas velocity  $v_g$  as a function of the fluid velocity  $v_f$  in the rest frame of the shock front. The dashed lines represent mechanically unstable transitions, whereas the solid lines show the mechanically stable FO shocks and normal shock waves. Thin lines correspond to a normal shock wave (Eq. (34)) and the thick ones correspond to the freeze-out shock (Eq. (33)). The circle has the coordinates  $(1/\sqrt{3}; 3 - 4/\sqrt{3})$  and the square has the coordinates  $(1/\sqrt{3}; 1/\sqrt{3})$ .

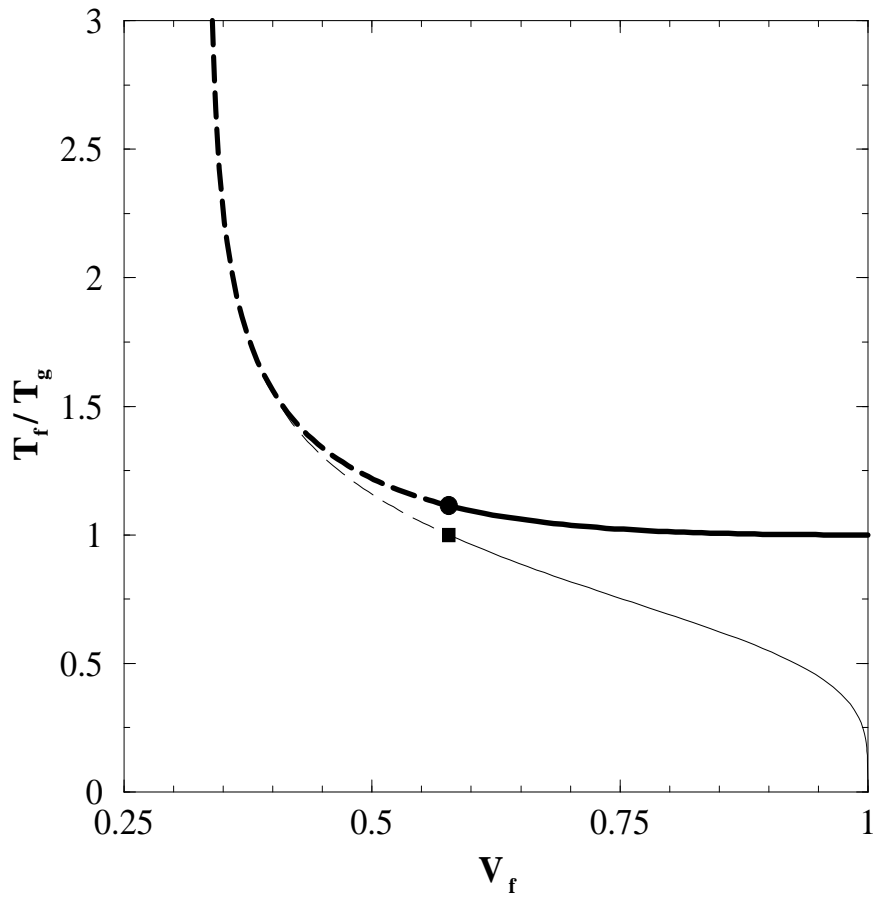


**Fig. 3.** Ratio of the temperatures on the both sides of the shock front,  $T_f/T_g$ , as a function of the fluid velocity  $v_f$  in the rest frame of the shock front. The legend corresponds to the Fig. 2. The circle has the coordinates  $[1/\sqrt{3}; (8/(3\sqrt{3}))^{1/4}]$  and the square has the coordinates  $(1/\sqrt{3}; 1)$ .



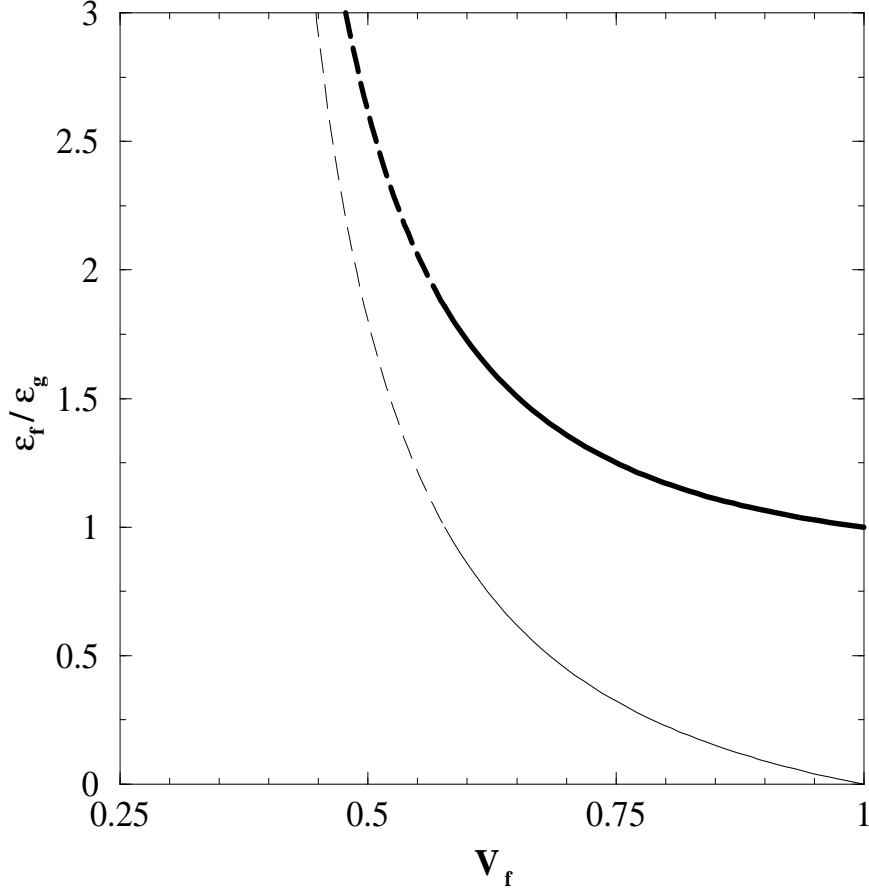


**Fig. 4.** Ratio of the energy densities on the both sides of the shock front, as a function of the fluid velocity  $v_f$  in the rest frame of the freeze-out shock front. The dashed lines represent mechanically unstable transitions, whereas the solid lines show the mechanically stable FO shocks and normal shock waves. Thin lines correspond to a normal shock wave and the thick ones correspond to the freeze-out shock. The energy density  $\varepsilon_g$  is given by Eq. (29) for the normal shock wave and for the gas of free particles after the FO shock it is  $T_g^{00}(v_g, T_g)|_{L.L.}$  defined by Eq. (35).

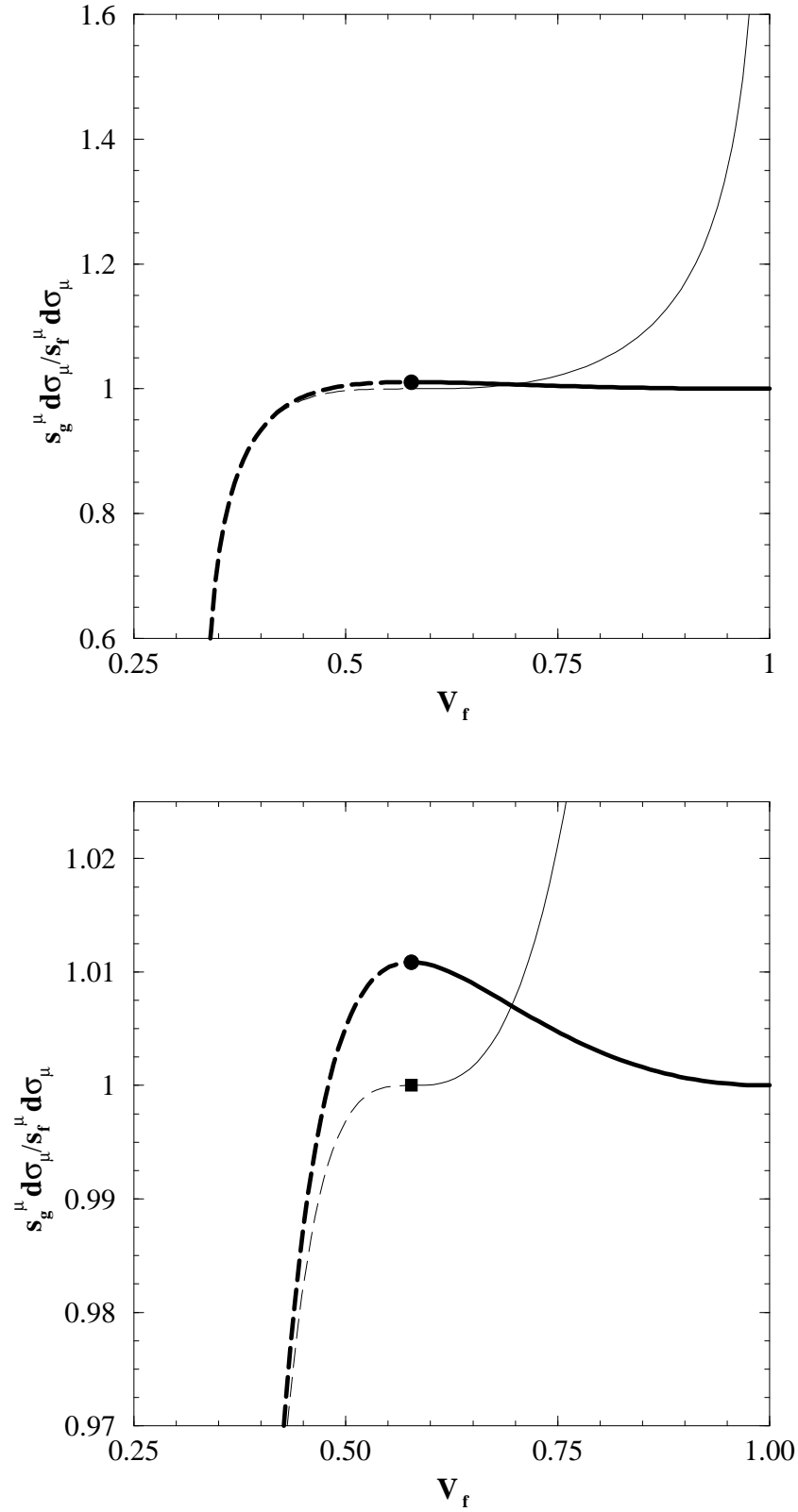


**Fig. 5.** Ratio of the entropies on the both sides of the shock front, as a function of the fluid velocity  $v_f$  in the rest frame of the shock front. The legend corresponds to the Fig. 2. The upper and lower panels differ by the vertical scale. The circle corresponds to the maximal entropy (analog of the Chapman-Jouguet point) in the freeze-out shock and it has the coordinates  $\left[1/\sqrt{3}; \left(\frac{9(3-\sqrt{3})}{4(\sqrt{3}+1)}\right)^{1/4}\right]$  and the square has the coordinates  $(1/\sqrt{3}; 1)$ .

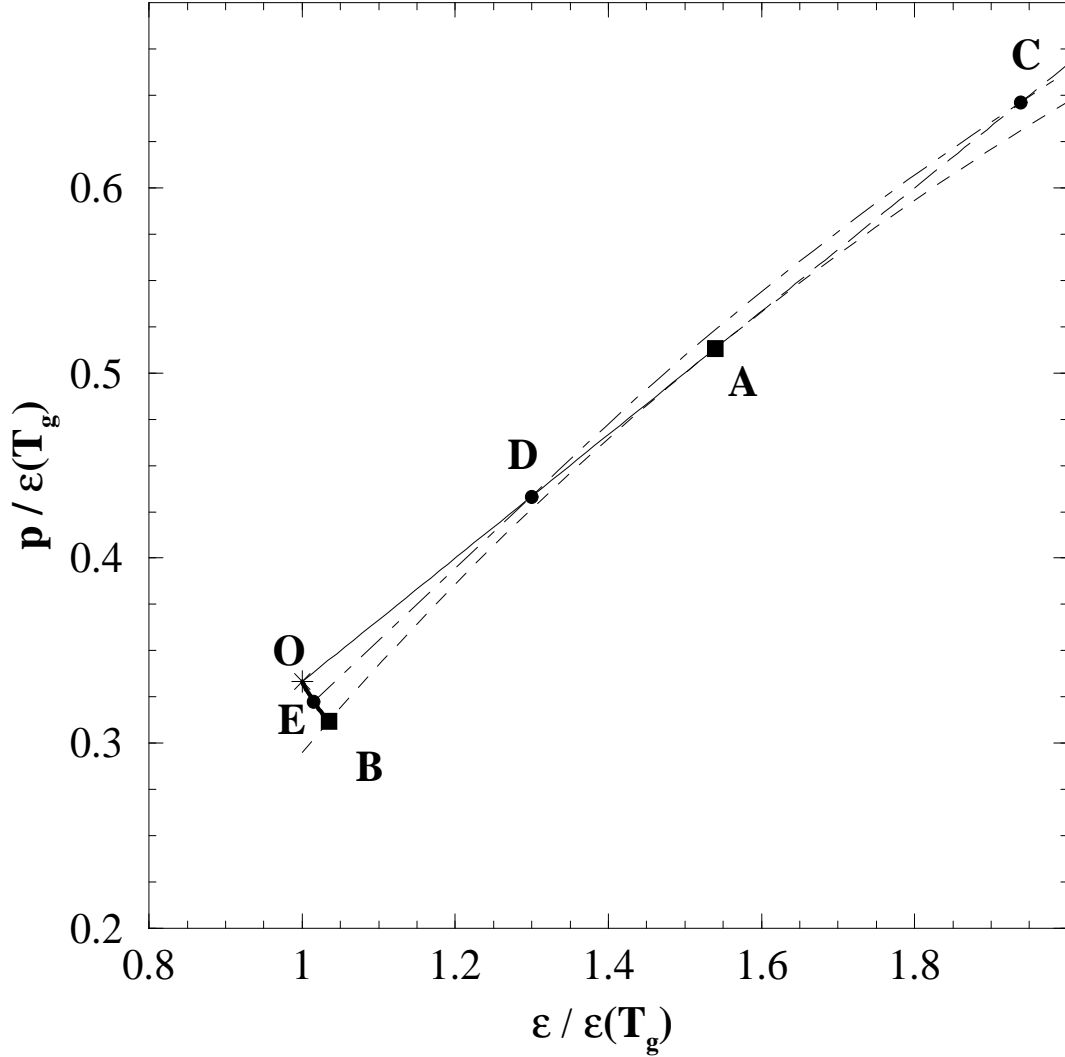


**Fig. 6.** Possible initial and final states in the  $\varepsilon - p$  plane for the freeze-out shock transitions. Initial fluid states are on the straight line  $p = \varepsilon/3$ . Each initial state on OA interval corresponds to the one point on curve OB of the final gas states in the FO shock (see text also). The initial fluid states of the unstable FO shock transitions are shown by the long dashed line. The critical curve  $p_{cr}(\varepsilon)$  for A $\rightarrow$ B FO shock (short dashed line) is a tangent to the line  $p = \varepsilon/3$  at the point A which is an analog of the Chapman-Jouguet point. The critical curve  $p_{cr}(\varepsilon)$  for C $\rightarrow$ E FO shock (dashed-dotted line) crosses the line  $p = \varepsilon/3$  at the point D.